Available online at www.sciencedirect.com
SCIENCE DIRECT®
Journal of Computational Physics 200 (2004) 654–669
JOURNAL OF COMPUTATIONAL PHYSICS
www.elsevier.com/locate/jcp

The shallow water equations in Lagrangian coordinates

J.L. Mead

Department of Mathematics, Boise State University, Boise, ID 83725-1555, USA

Received 1 December 2003; received in revised form 16 April 2004; accepted 29 April 2004
Available online 24 June 2004

Abstract

Recent advances in the collection of Lagrangian data from the ocean and results about the well-posedness of the primitive equations have led to a renewed interest in solving flow equations in Lagrangian coordinates. We do not take the view that solving in Lagrangian coordinates equates to solving on a moving grid that can become twisted or distorted. Rather, the grid in Lagrangian coordinates represents the initial position of particles, and it does not change with time. We apply numerical methods traditionally used to solve differential equations in Eulerian coordinates, to solve the shallow water equations in Lagrangian coordinates. The difficulty with solving in Lagrangian coordinates is that the transformation from Eulerian coordinates results in solving a highly nonlinear partial differential equation. The non-linearity is mainly due to the Jacobian of the coordinate transformation, which is a precise record of how the particles are rotated and stretched. The inverse Jacobian must be calculated, thus Lagrangian coordinates cannot be used in instances where the Jacobian vanishes. For linear (spatial) flows we give an explicit formula for the Jacobian and describe the two situations where the Lagrangian shallow water equations cannot be used because either the Jacobian vanishes or the shallow water assumption is violated. We also prove that linear (in space) steady state solutions of the Lagrangian shallow water equations have Jacobian equal to one. In the situations where the shallow water equations can be solved in Lagrangian coordinates, accurate numerical solutions are found with finite differences, the Chebyshev pseudospectral method, and the fourth order Runge–Kutta method. The numerical results shown here emphasize the need for high order temporal approximations for long time integrations.

Keywords: Lagrangian coordinates; Shallow water equations; Jacobian; Finite differences; Chebyshev pseudospectral; Runge–Kutta

1. Introduction

There are two distinct ways to specify a flow field. The typical approach is Eulerian where the flow quantities are defined as functions of space and time. It gives a picture of the spatial distribution of the flow quantities at each instant during motion [1] and the fluid motions and properties are described at fixed points. In this reference frame, one studies the individual spatial positions, regardless of *what* particles reach those positions at a given instant of time [11].

E-mail addresses: jmead@boisestate.edu, mead@math.boisestate.edu (J.L. Mead).

0021-9991/$ - see front matter
doi:10.1016/j.jcp.2004.04.014

Alternatively, we can use the Lagrangian description where the particles are identified by the positions they occupy at a given instant of time [11]. The Lagrangian solution has the future positions of all fluid elements with respect to their position at some initial time. The outcome of the Eulerian and Lagrangian approaches are equivalent if the total information about the entire body can be obtained [11].

Lagrangian coordinates have been neglected for different reasons. One reason is that scientists have typically only made Eulerian measurements and the Eulerian statistics are not related to Lagrangian ones in a simple way [15]. A second reason is that a Lagrangian specification is useful only in certain special contexts and it leads to a cumbersome analysis [1]. Thirdly, it is perceived that Lagrangian coordinates are a moving coordinate system and the grid can become twisted and distorted.

With advances in satellite monitoring, scientists are now collecting vast amounts of Lagrangian data in the ocean [7,10]. These data are collected from floats or drifters that remain in the ocean and transmit their information by satellite. Using these data in ocean models is a challenge because the models are written in Eulerian coordinates. Thus the first two reasons for not using Lagrangian coordinates given in the previous paragraph are not valid in this context. As a response to the third reason, we offer a different viewpoint of solving in Lagrangian coordinates. In Lagrangian coordinates the "grid" represents the initial position of the particles, which does not become twisted and distorted. The subsequent positions of the particles are calculated by solving a highly nonlinear partial differential equation (which is the result of the coordinate transformation) and the difficulty in solving in Lagrangian coordinates is not that the grid can become distorted, but that one needs to solve highly nonlinear equations. The nonlinearity is mainly due to the Jacobian of the transformation, which is a precise record of how the particles are rotated and stretched. Here, we begin a better understanding of solving in Lagrangian coordinates by analyzing the behavior of the highly nonlinear terms for simple flows. Solving these equations numerically adds challenges, but we hope to use numerical methods that accurately describe the physical situation that occurs.

A more theoretical reason for studying the Lagrangian viewpoint comes from results in [2] about the well-posedness of the primitive equations in an open domain. A problem occurs in the vertical direction when using Eulerian coordinates, because the flow can vary between subcritical and supercritical flow. One way to ensure uniqueness of solutions is to apply boundary conditions mode by mode, but this is not practical. Alternatively, the author's in [2] show that uniqueness of solutions can be guaranteed in the open ocean if the equations are solved on moving particles. Essentially, every mode is subcritical on the moving particles because vorticity is conserved on fluid particles. Thus when we solve the primitive equations in an open domain on moving particles (or Lagrangian coordinates), the boundary conditions do not need to be applied mode by mode.

Lagrangian coordinates have not been completely abandoned. It has be noted that the nonlinear advective terms in the governing equations for atmospheric modeling are greatly simplified in Lagrangian coordinates. However, in this setting, the pressure gradient and viscous terms become more nonlinear. Semi-Lagrangian methods [14] take all of this under consideration and only use Lagrangian coordinates for the advective terms, while still calculating the pressure gradient terms on an Eulerian grid. Thus an accurate interpolation scheme is critical to the success of semi-Lagrangian methods.

The arbitrary Lagrangian Eulerian method, (ALE) [8], temporarily computes the entire governing equations in Lagrangian coordinates. Then at some arbitrary point in time the solution is interpolated and the governing equations are computed in Eulerian coordinates. If one chooses to interpolate the solution at nearly every time-step, the approach is then similar to the semi-Lagrangian method described in the previous paragraph.

Lagrangian coordinates are not the only way to follow particles. Unified coordinates [16] follow pseudo-particles, which are usually slower than the Lagrangian particles. The speed of the particles depends on the choice of a given parameter and the authors suggest that a purely Lagrangian flow is not a good choice.

There are no benchmark problems for Lagrangian coordinates, nor is there a standard way of presenting solutions. Here, we develop the convention of plotting the trajectories, or the solution of the given

differential equation at all points in space for all time. Obviously, the greatest error is at the final time and that is where we determine their accuracy, but the power of Lagrangian solution is its temporal evolution. The problems we solve here include the following linear trajectories: center, spiral, source and sink. We also solve a nonlinear problem with a solution that combines all of these forms.

In Section 2, we state the advective form of the shallow water equations in Lagrangian coordinates. In Section 2.2, we investigate the asymptotic behavior of the shallow water equations in Lagrangian form for linear flows. Then in Section 4, we describe the numerical methods and state the test problems with their numerical results. The conclusions are in Section 3.

2. Lagrangian shallow water equations

2.1. Derivation of the equations

The shallow water equations can be written in different forms and here we use the advective form. In Eulerian coordinates, the horizontal momentum equations are:

$$\frac{\mathrm{D}u}{\mathrm{D}t} - fv = -g\frac{\partial h}{\partial x}, \tag{1}$$

$$\frac{\mathrm{D}v}{\mathrm{D}t} + fu = -g\frac{\partial h}{\partial y}, \tag{2}$$

with the material derivative

$$\frac{\mathrm{D}}{\mathrm{D}t} = \frac{\partial}{\partial t} + u\frac{\partial}{\partial x} + v\frac{\partial}{\partial y}.$$

The mass continuity equation is

$$\frac{\mathrm{D}h}{\mathrm{D}t} + h\left(\frac{\partial u}{\partial x} + \frac{\partial v}{\partial y}\right) = 0. \tag{3}$$

The horizontal velocities u and v are in the East/West and North/South directions, respectively. In the ocean (the viewpoint adopted here) h is the depth of a surface with constant density, while in the atmosphere it is the height of the free surface above sea level. In addition, f is the Coriolis parameter and g is the gravitational constant. An illustration of the ocean viewpoint is given in Fig. 1.

In Eulerian coordinates, the velocities u and v, and the depth h, are given at fixed points in space (x, y). In Lagrangian coordinates, the velocities and depth are given on moving particles with positions $(x(a, b, t), y(a, b, t))$ at time t, where (a, b) are the initial positions of the particles. In Lagrangian coordi-

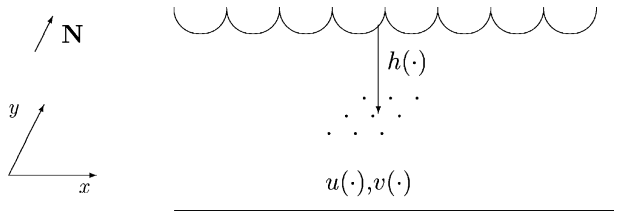

Fig. 1. Eulerian shallow water.

nates, the positions of the particles are calculated at all points in time from which the velocities at these positions can be inferred. The depth of the moving particles are calculated by solving the appropriate continuity equation in Lagrangian coordinates, i.e., (9). The Lagrangian view of the shallow water equations in given in Fig. 2.

The coordinate transformation from Eulerian $u(x,y,t), v(x,y,t), h(x,y,t)$ to Lagrangian $x(a,b,t)$, $y(a,b,t), h(a,b,t)$ follows:

$$u(x,y,t) = \frac{\partial}{\partial t}x(a,b,t), \tag{4}$$

$$v(x,y,t) = \frac{\partial}{\partial t}y(a,b,t). \tag{5}$$

The spatial derivatives in the two coordinate systems are related via

$$\frac{\partial}{\partial a} = \frac{\partial}{\partial x}\frac{\partial x}{\partial a} + \frac{\partial}{\partial y}\frac{\partial y}{\partial a},$$

$$\frac{\partial}{\partial b} = \frac{\partial}{\partial x}\frac{\partial x}{\partial b} + \frac{\partial}{\partial y}\frac{\partial y}{\partial b}.$$

The Jacobian of the transformation is

$$J = \frac{\partial(x,y)}{\partial(a,b)} \equiv \frac{\partial x}{\partial a}\frac{\partial y}{\partial b} - \frac{\partial y}{\partial b}\frac{\partial x}{\partial b} \tag{6}$$

and to change from Eulerian spatial derivatives to Lagrangian we use

$$\frac{\partial}{\partial x} = J^{-1}\left(\frac{\partial}{\partial a}\frac{\partial y}{\partial b} - \frac{\partial}{\partial b}\frac{\partial y}{\partial a}\right),$$
$$\frac{\partial}{\partial y} = J^{-1}\left(\frac{\partial x}{\partial a}\frac{\partial}{\partial b} - \frac{\partial x}{\partial b}\frac{\partial}{\partial a}\right).$$

Note that in Lagrangian coordinates differentiation with respect to time is performed by following the motion of a given particle, thus the material derivative D/Dt is equivalent to the partial derivative $\partial/\partial t$ [11]. Thus, the Lagrangian shallow water equations in Cartesian coordinates have momentum equations

$$\frac{\partial^2 x}{\partial t^2} - f\frac{\partial y}{\partial t} = -g\frac{\partial(h,y)}{\partial(a,b)}J^{-1}, \tag{7}$$

$$\frac{\partial^2 y}{\partial t^2} + f\frac{\partial x}{\partial t} = -g\frac{\partial(x,h)}{\partial(a,b)}J^{-1}. \tag{8}$$

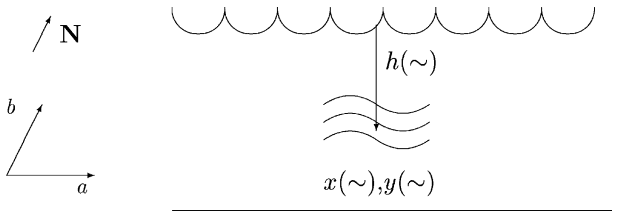

Fig. 2. Lagrangian shallow water.

The continuity equation is transformed similarly. We begin by transforming the spatial derivatives in (3)

$$\frac{\partial u}{\partial x}+\frac{\partial v}{\partial y}=\frac{\partial}{\partial x}\left(\frac{\partial x}{\partial t}\right)+\frac{\partial}{\partial y}\left(\frac{\partial y}{\partial t}\right)=J^{-1}\frac{\partial}{\partial t}J.$$

Thus the continuity equation in Lagrangian coordinates is

$$\frac{\partial h}{\partial t}+hJ^{-1}\frac{\partial}{\partial t}J=0$$

or

$$\frac{\partial}{\partial t}(hJ)=0.$$

One advantage of using Lagrangian coordinates is that the continuity equation can by solved exactly, i.e.,

$$h=(hJ)_0J^{-1}, \tag{9}$$

where $(hJ)_0$ is the initial value of hJ. The full derivation of (7)–(9) can be found in [6].

In [2], the authors show that uniqueness of solutions of the shallow water equations on moving particles is guaranteed if appropriate boundary conditions are used, and they give some numerical results from the Lagrangian form. Here, we more rigorously investigate the dynamical behavior and the numerical solution of (7)–(9).

To fully appreciate the underlying dynamical system and its nonlinearities we rewrite the second-order derivative system (7) and (8) as a first-order system:

$$\frac{\partial x}{\partial t}=u, \tag{10}$$

$$\frac{\partial y}{\partial t}=v, \tag{11}$$

$$\frac{\partial u}{\partial t}=fv-g\frac{(h,y)}{\partial(a,b)}J^{-1}, \tag{12}$$

$$\frac{\partial v}{\partial t}=fu-g\frac{\partial(x,h)}{\partial(a,b)}J^{-1}. \tag{13}$$

2.2. Asymptotic behavior for linear flows

In this section, we investigate the asymptotic behavior of the Lagrangian shallow water model (9)–(13) with initial conditions

$$x(a,b,0)=a,\quad y(a,b,0)=b, \tag{14}$$

$$u(a,b,0)=u_0,\quad v(a,b,0)=v_0, \tag{15}$$

$$h(a,b,0)=h_0. \tag{16}$$

One of the barriers to using Lagrangian coordinates is that numerical calculations will break down as $J \to 0$. Since the Lagrangian shallow water equations are highly nonlinear, we will not determine the stability of specific numerical methods used to solve them. Rather we will assume that traditional Eulerian numerical methods will follow the flow accurately when J is not near zero. We will however, determine theoretically the circumstances under which $J \to 0$ and more completely, the circumstances under which the shallow water equations in Lagrangian coordinates are valid.

Recall that when using the shallow water equations, it is assumed that the depth of the isopycnal, i.e., $h(a,b,t)$, is slowly varying with respect to spatial position. That is, the variation of h over horizontal distances of order h is negligible [1]. Here, we have an explicit formula for h, i.e., (9), thus we know that as $t \to \infty$ if J^{-1} approaches infinity, then the depth h approaches infinity, and the shallow water assumption is violated. In addition, if the depth h is large initially and J^{-1} approaches 0, the shallow water assumption will again be violated.

To understand the circumstances under which the shallow water assumption is violated, we look at the situation when the underlying dynamical system

$$\frac{\partial x}{\partial t} = u, \quad \frac{\partial y}{\partial t} = v$$

is linear with respect to x and y and has constant coefficients, i.e.,

$$u = c_1 x + c_2 y, \tag{17}$$

$$v = c_3 x + c_4 y. \tag{18}$$

Theorem 1. *If u and v in the solution of* (9), (10)–(13), (14)–(16) *take the form* (17) and (18), *then the Jacobian J takes the form*

$$J = \mathrm{e}^{(\lambda_1+\lambda_2)t}, \tag{19}$$

where λ_1 and λ_2 are the (*not necessarily distinct*) *real parts of the eigenvalues of the matrix*

$$A = \begin{pmatrix} c_1 & c_2 \\ c_3 & c_4 \end{pmatrix}. \tag{20}$$

Consequently

$$\lim_{t\to\infty} h = \lim_{t\to\infty} h_0 J^{-1} = \begin{cases} h_0 & \text{if } \lambda_1+\lambda_2 \ (\text{saddle}, \ \lambda_1 = \lambda_2 = 0), \\ 0 & \text{if } \lambda_1+\lambda_2 > 0 \ (\text{saddle}, \ \text{source}), \\ \infty & \text{if } \lambda_1+\lambda_2 < 0 \ (\text{saddle}, \ \text{sink}). \end{cases}$$

Proof. The Jacobian J is defined

$$J = \frac{\partial x}{\partial a}\frac{\partial y}{\partial b} - \frac{\partial x}{\partial b}\frac{\partial y}{\partial a},$$

where $x(a,b,t)$ and $y(a,b,t)$ are solutions of

$$\frac{\partial x}{\partial t} = c_1 x + c_2 y, \tag{21}$$

$$\frac{\partial x}{\partial t} = c_3 x + c_4 y, \tag{22}$$

with initial conditions $x(a,b,0) = a$ and $y(a,b,0) = b$.

The linearity assumption implies the problem is a standard two-dimensional, constant coefficient, ordinary differential equation (ODE) system (21) and (22) with equilibrium solution at the origin. As can be found in any ODE textbook there are three cases: real and distinct eigenvalues (source, sink, saddle), real repeated eigenvalue or two imaginary eigenvalues (spiral or center). By using the appropriate (x,y) solution for each case, it is easy to see J has the form given by (19). Given explicit values for J, the asymptotic behavior of h is found from (9). □

The following are consequences of Theorem 1:

- Sources, sinks or saddles: For long time integrations, the shallow water assumption will be violated if there is a sink or the saddle where h approaches infinity, because h will have large variation. In addition, the shallow water assumption will be violated in long time integrations if the initial depth h_0 is large and there is a source or the type of saddle where h approaches 0. In all other cases, a stable, accurate, numerical method will be able to calculate solutions for long time periods.
- Centers: The eigenvalues of (20) have zero real part, thus $J = 1$. In addition the solutions in the (x,y) plane remain valid as $t \to \infty$. Thus, a stable, accurate, numerical method will be able to calculate solutions for long time periods.
- Spiral sources or sinks: Both the real and imaginary parts of (20) are nonzero and the situation is similar to a source or sink. That is, there is a problem with long time integrations if there is a spiral sink, while if the initial depth is large, a problem if there is a spiral source. However, in the other cases a stable, accurate, numerical method will be able to calculate solutions for long time periods.

Theorem 2. *Steady state solutions of the Lagrangian shallow water equations* (7)–(9), (14)–(16) *which satisfy* (17) and (18) *and satisfy*

$$\frac{\partial u}{\partial t} = 0, \quad \frac{\partial v}{\partial t} = 0, \tag{23}$$

have corresponding Jacobian

$$J = 1.$$

Proof. Conditions (12) and (13) and (23) imply

$$\frac{\partial h}{\partial a} = \frac{f}{g}\left(\frac{\partial x}{\partial a} v - \frac{\partial y}{\partial a} u\right), \tag{24}$$

$$\frac{\partial h}{\partial b} = \frac{f}{g}\left(\frac{\partial x}{\partial b} v - \frac{\partial y}{\partial b} u\right). \tag{25}$$

We can construct an h which satisfies (24) and (25) if

$$\frac{\partial x}{\partial a}\frac{\partial v}{\partial b} - \frac{\partial y}{\partial a}\frac{\partial u}{\partial b} = \frac{\partial x}{\partial b}\frac{\partial v}{\partial a} - \frac{\partial y}{\partial b}\frac{\partial u}{\partial a}. \tag{26}$$

Using (10) and (11) and (17) and (18) in (26) we get that $c_1 = -c_4$.

We also note the following four conditions for steady state solutions:

$$\frac{\partial x}{\partial t} = c_1 x + c_2 y, \quad c_1 \frac{\partial x}{\partial t} + c_2 \frac{\partial y}{\partial t} = 0,$$
$$\frac{\partial y}{\partial t} = c_3 x + c_4 y, \quad c_3 \frac{\partial x}{\partial t} + c_4 \frac{\partial y}{\partial t} = 0.$$

Assuming all of the coefficients are non-zero, we get that $c_1 c_4 = c_2 c_3$. In this case, the matrix A is singular, has zero eigenvalues, and thus $J = 1$. When the coefficients may be zero, all possible steady state solutions are given in Table 1, and have corresponding Jacobian equal to one. □

We conclude this section by stating that if we discretize the Lagrangian shallow water equations equations, i.e. (7)–(9), and solutions are of the form (17) and (18) then valid solutions can be found for long time periods in all but the following two cases

- The sum of the real parts of the eigenvalues of (20) is strictly negative, thus the solution of the Lagrangian shallow water equations is a sink, spiral sink or saddle. In this case as $t \to \infty$ either all or a significant portion of the particles converge together, the isopycnal moves infinitely deep, and the Jacobian vanishes.
- The initial depth h is large and the sum of the real parts of the eigenvalues of (20) is strictly positive, thus the solution of the Lagrangian shallow water equations is a source, spiral source or saddle. In this case as $t \to \infty$ either all or a significant portion of the particles diverge, the isopycnal moves to the surface, and the shallow water assumption is violated.

3. Numerical experiments

3.1. Numerical methods

There are no standard numerical techniques for solving the Lagrangian shallow water Eqs. (7)–(9). We chose to compare numerical solutions from both high and low order methods. For the spatial derivative approximations we used a finite difference method for the low order method because of the ease of implementation, and the Chebyshev pseudospectral method for the high order method because of its spectral accuracy. For the temporal derivative approximations we again chose finite differences for the low order approximation, and a fourth order Runge–Kutta method for the high order method.

There are a variety of finite difference schemes that can be used, however due to the highly nonlinear nature of the equations analysis of different schemes is not straightforward. In this preliminary work we simply choose second order centered differences in time and space with one sided differences at the boundary. In Lagrangian coordinates the spatial derivative approximation with finite differences is

$$\frac{\partial}{\partial a} x^k_{i,j} = \frac{x^k_{i+1,j} - x^k_{i-1,j}}{2\Delta a},$$

Table 1
Linear steady state solutions with zero coefficients

A	$\begin{pmatrix} 0 & 0 \\ 0 & 0 \end{pmatrix}$	$\begin{pmatrix} 0 & c_2 \\ 0 & 0 \end{pmatrix}$	$\begin{pmatrix} 0 & 0 \\ c_3 & 0 \end{pmatrix}$	$\begin{pmatrix} 0 & 0 \\ c_3 & c_4 \end{pmatrix}$	$\begin{pmatrix} c_1 & c_2 \\ 0 & 0 \end{pmatrix}$
Solution	$x = a$ $y = b$	$x = a + c_2 bt$ $y = b$	$x = a$ $y = b + c_3 at$	$x = a$ $y = -\frac{c_3}{c_4} a = b$	$x = -\frac{c_1}{c_2} b = a$ $y = b$

and similarly for $\partial x/\partial b$, $\partial y/\partial a$, and $\partial y/\partial b$. The low order temporal discretization in Lagrangian coordinates is

$$\frac{\partial^2}{\partial t^2} x_{i,j}^k = \frac{x_{i,j}^{k+1} - 2x_{i,j}^k + x_{i,j}^{k-1}}{(\Delta t)^2}.$$

The Chebyshev pseudospectral method is a truncated global approximation

$$x(a) \approx \sum_{j=0}^{N} c_j T_j(a),$$

where the basis functions $T_j(a)$ are the set of orthogonal Chebyshev polynomials

$$T_j(a) = \cos(j \cos^{-1} a).$$

The collocation method is used to calculate the coefficients $\{c_j\}$, that is, the approximation is exact at the Chebyshev points $a_k = \cos(\pi k/N)$, $k = 0, \ldots, N$. This method gives highly accurate approximations for the solution of partial differential equations [3,4], and has been widely used and studied, e.g. [5,9,12,13].

The spatial derivative is approximated by considering that there are unique Lagrange polynomials $l_j(a)$ of degree N [3] such that

$$x(a) \approx \sum_{j=0}^{N} x(a_j) l_j(a).$$

Thus

$$\frac{d}{da} x(a) \approx \sum_{j=0}^{N} x(a_j) \frac{\mathrm{d}}{\mathrm{d}a} l_j(a),$$

or for $x = (x(a_0), \ldots, x(a_N))^{\mathrm{T}}$

$$\frac{\partial x}{\partial a} = \mathrm{D}x,$$

where

$$D_{ij} = \frac{\mathrm{d}}{\mathrm{d}a} l_j(a)|_{a=a_i}.$$

Note that the matrix D is dense, while it is sparse for the finite difference method. A three point centered difference, for example, leads to a tridiagonal matrix D in one-dimensional applications. Pseudospectral methods can also be seen as the limits of finite difference methods of increasingly higher order [4]. Here we use an FFT algorithm to compute the derivative [3].

In the two-dimensional problem with N points in the East/West direction and M points in the North/South direction $x(a, b)$ is represented by a matrix of the form

$$X = \begin{pmatrix} x(a_0, b_0) & x(a_0, b_1) & \ldots & x(a_0, b_M) \\ x(a_1, b_0) & x(a_1, b_1) & \ldots & x(a_1, b_M) \\ \vdots & \vdots & \vdots & \vdots \\ x(a_N, b_0) & x(a_N, b_1) & \ldots & x(a_N, b_M) \end{pmatrix}.$$

The spatial derivatives can then be represented

$$\left(\frac{\partial x}{\partial a}\right)_{ij} = \sum_{k=0}^{N} D_{ik} X_{kj},$$
$$\left(\frac{\partial x}{\partial b}\right)_{ij} = \sum_{k=0}^{N} D_{jk} X_{ik}$$

for $i = 1, \ldots, N-1$ and $j = 1, \ldots, M-1$.

The high order temporal integration is done with the classical fourth order Runge–Kutta method, and the second order time derivative is written as a first order system, i.e. (10)–(13).

Three different combinations of numerical methods were used: (1) finite difference in space and time (FD/FD), (2) finite difference in space and Runge–Kutta in time (FD/RK), and (3) Chebyshev pseudospectral in space and Runge–Kutta in time (CPS/RK). In most of the test problems, the spatial derivatives are of simple linear functions, thus the accuracy of the temporal discretization is more important than the accuracy of the spatial discretization. In these cases good accuracy is obtained with a small number of spatial grid points and increasing the number of grid points does not decrease the error. Also noteworthy is the fact that a small time step was needed for both the low and high order spatial discretization. The is due to the highly nonlinear time integration.

3.2. Test problems

Shallow water theory states that the range of the depth $h(a, b, t)$ should be much smaller than the size of the domain $[a_0, a_n] \times [b_0, b_n]$. In these simulated examples we used the spatial range $[-1, 1] \times [-1, 1]$ in meters and initial depth $h_0 = 0.002$ m. We applied the initial conditions (14)–(16), and the magnitude of the initial velocities are consistently 1 m/s. Results are shown at $T = 1$, 2 s. In some cases, the velocities and depth increase, while in others they decrease.

Boundary conditions were specified for x on the East/West boundary, for y on the North/South boundaries, and for h at all boundaries. These are the open boundary conditions that ensure a unique solution for the shallow water equations on moving particles, as proved in [2].

For each test problem, appropriate forcing terms were added to the Lagrangian shallow water equations to ensure that the test problem was an exact solution. However, in the case of the center, an exact solution was found without adding a forcing term. The exact solutions for each of the five problems are given below and plotted in Figs. 3–5.

The errors are measured at the final integration time step and they are calculated

$$e_\infty(x, y) = \frac{\max_{\text{all } a,b} \sqrt{(x(a,b) - x_T(a,b))^2 + (y(a,b) - y_T(a,b))^2}}{\max_{\text{all } a,b} \sqrt{x_T(a,b)^2 + y_T(a,b)^2}},$$

$$e_\infty(h) = \frac{\max_{\text{all } a,b} |h(a,b) - h_T(a,b)|}{\max_{\text{all } a,b} |h_T(a,b)^2|},$$

- *Center*

$$x = a\cos t + b\cos t,$$
$$y = -a\sin t + b\cos t,$$
$$h = \frac{1-f}{2g}(a^2 + b^2 - \max(a^2 + b^2)) + h_0.$$

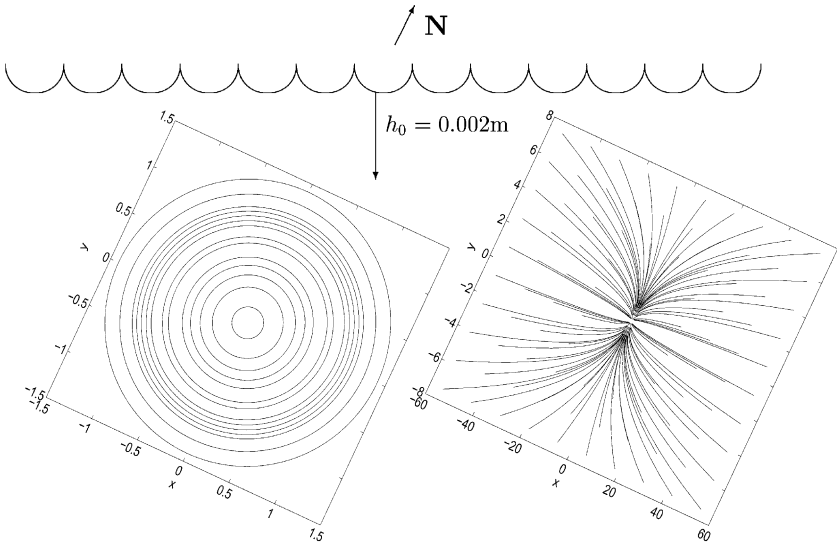

Fig. 3. Two second trajectory solutions of Lagrangian shallow water equations with $N, M = 10$, the center (left) and source (right) test problems.

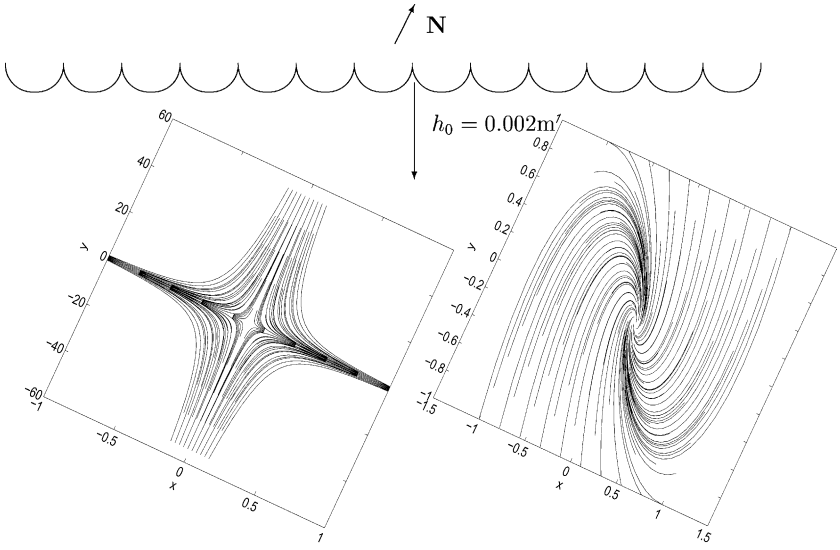

Fig. 4. Two second trajectory solutions of Lagrangian shallow water equations with $N, M = 10$, the saddle (left) and spiral sink (right) test problems.

Errors are shown in Table 2, and we see that the solution from the high order method (CPS/RK) is significantly better than that from the other two methods. The depth in this problem is quadratic in both a and b, thus the high order spatial approximation (CPS) increases the accuracy considerably. On the other hand, adding a high order temporal approximation (RK) to the finite difference method does not compensate for the inaccuracies in the spatial finite difference method.

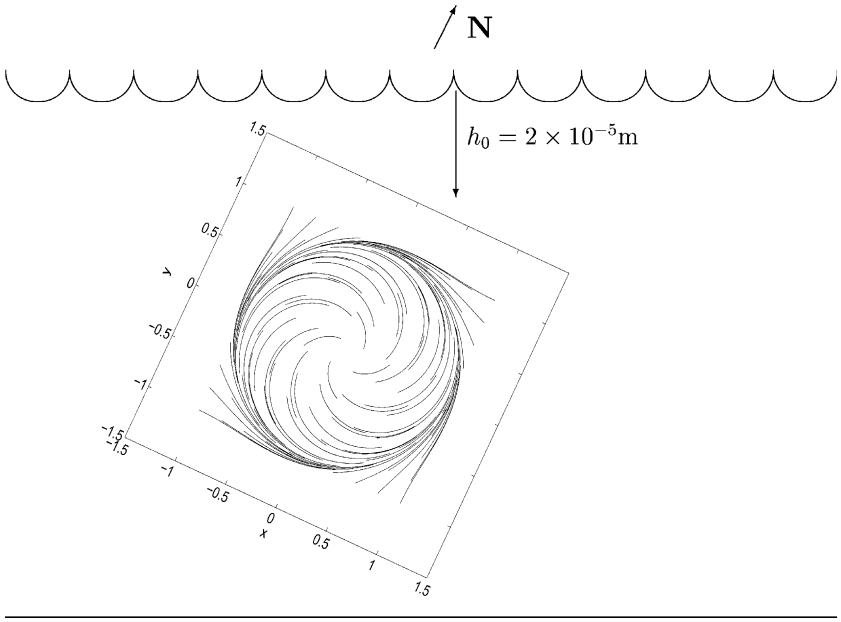

Fig. 5. Two second trajectory solutions of Lagrangian shallow water equations with $N, M = 10$, the nonlinear test problem.

Table 2
Error in the solution of the Lagrangian shallow water equations for the center test problem

Method	N, M	Δt	T	$e_\infty(x, y)$	$e_\infty(h)$
FD/FD	10	1E − 03	1	1.6E − 02	3.0E − 02
			2	3.1E − 01	4.5E + 00
FD/RK	10	1E − 03	1	1.6E − 02	2.8E − 02
			2	2.5E − 01	1.2E + 01
CPS/RK	6	1E − 03	1	2.6E − 14	9.2E − 14
			2	1.1E − 12	5.3E − 12

Table 3
Error in the FD/FD solution of the Lagrangian shallow water equations for the center test problem at $T = 1$

N, M	10	10	10	14	20
Δt	1E − 03	1E − 04	1E − 05	1E − 05	1E − 05
$e_\infty(x, y)$	1.58E − 02	1.57E − 02	1.57E − 02	1.28E − 02	1.24E − 02
$e_\infty(h)$	3.04E − 02	3.14E − 02	3.15E − 02	3.70E − 02	5.68E − 02

Results for different grids N, M and temporal samplings Δt are given in Table 3. There we see that increasing the number of grid points and/or decreasing the step size does not improve the accuracy of the solution with FD/FD. This lack of improvement with the finite difference method occurs here and in the nonlinear example where the exact solution for h is nonlinear in a and b.

• *Source*

$$x = a\mathrm{e}^{2t},$$
$$y = b\mathrm{e}^{t},$$
$$h = h_0(a+b).$$

Errors are shown in Table 4 and there is significant improvement when the high order temporal approximation (RK) is used, because the source solution is growing exponentially in time. Here h is a linear function of a and b, thus the spatial derivative approximation is good even with the low order method (FD).

The computational cost of each FD spatial derivative approximation is $2M$ or $2N$ depending on which derivative is approximated (in these examples $M = N$), while the computational cost of the CPS spatial derivative approximation with the FFT is $2N + 2N\log N$ (or $2M + 2M\log M$). There are six spatial derivatives which need to be approximated at each time step, and using the fourth order Runge–Kutta method there are four function evaluation for each spatial derivative at each time step. At each time step the cost of the spatial derivative approximations with the FD method is 480 when $N = M = 10$, while with the CPS method it is 512 when $N = M = 6$. Thus FD/RK and CPS/RK give results with the same order of accuracy and no significant difference in computational cost.

The error in the FD/FD method improves when the time step is reduced, and these results are given in Table 5. However, the results with FD/FD are still not as good as those with FD/RK and the computational cost of FD with time step of 10^{-6} is greater than the cost of RK with time step of 10^{-3}.

• *Saddle*

$$x = a\mathrm{e}^{-t},$$
$$y = b\mathrm{e}^{2t},$$
$$h = h_0(a+b)\mathrm{e}^{-t}.$$

Errors are given in Table 6 and we see that the results are similar to those for the source. The spatial derivatives are of linear functions, so dramatic improvement is obtained simply by adding a high order numerical method in time.

Table 4
Error in the solution of the Lagrangian shallow water equations for the source test problem

Method	N, M	Δt	T	$e_\infty(x,y)$	$e_\infty(h)$
FD/FD	10	1E − 03	1	2.0E − 04	4.4E − 04
			2	5.8E − 05	2.0E − 04
FD/RK	10	1E − 03	1	1.4E − 14	2.1E − 14
			2	1. 1E − 13	2.3E − 13
CPS/RK	6	1E − 03	1	1.3E − 14	2.6E − 14
			2	1.2E − 13	2.7E − 13

Table 5
Error in the FD/FD solution of the Lagrangian shallow water equations for the source test problem at $T = 1$, $N = M = 10$

Δt	1E − 03	1E − 04	1E − 05	1E − 06
$e_\infty(x,y)$	2.04E − 04	2.04E − 05	2.04E − 06	2.03E − 07
$e_\infty(h)$	4.44E − 04	4.44E − 05	4.44E − 06	4.45E − 07

Table 6
Error in the solution of the Lagrangian shallow water equations for the saddle test problem

Method	N, M	Δt	T	$e_\infty(x,y)$	$e_\infty(h)$
FD/FD	10	1E − 03	1	2.2E − 04	1.7E − 03
			2	6.0E − 05	1. 1E − 02
FD/RK	10	1E − 03	1	1.6E − 14	3.7E − 14
			2	1. 1E − 13	3.7E − 13
CPS/RK	6	1E − 03	1	1.3E − 14	4.3E − 14
			2	1.2E − 13	5.3E − 13

- *Spiral sink*

$$x = \mathrm{e}^{-t}(a\cos t + (a+b)\sin t),$$
$$y = \mathrm{e}^{-t}(b\cos t - (2a+b)\sin t),$$
$$h = h_0(a+b)\mathrm{e}^{2t}.$$

Errors are in Table 7 and we see similar behavior as the source and saddle at time $T = 1$. However, at $T = 2$ the solutions become unreliable for all methods. This is because the depth h grows exponentially in time and thus the shallow water assumption is violated. At time $T = 2$ the depth has grown to 54 times its original size, so the range of h is no longer significantly smaller than the spatial scale. We are able to obtain more accurate solutions and integrate for longer time periods if we take a smaller value for h. In Table 8 we show results when $h_0 = 2 \times 10^{-5}$.

Table 7
Error in the solution of the Lagrangian shallow water equations for the spiral sink test problem, $h_0 = 0.002$ m

Method	N, M	Δt	T	$e_\infty(x,y)$	$e_\infty(h)$
FD/FD	10	1E − 03	1	5.2E − 03	9.5E − 02
			2	1.2E + 02	7.8E − 01
FD/RK	10	1E − 03	1	6.0E − 14	4.7E − 13
			2	5.4E + 01	7.6E − 01
CPS/RK	6	1E − 03	1	1.3E − 13	7.0E − 13
			2	6.1E + 01	8.2E − 01

Table 8
Error in the solution of the Lagrangian shallow water equations for the spiral sink test problem, $h_0 = 0.00002m$

Method	N, M	Δt	T	$e_\infty(x,y)$	$e_\infty(h)$
FD/FD	10	1E − 03	1	2.6E − 03	2.3E − 02
			2	2.9E − 02	3.7E − 01
FD/RK	10	1E − 03	1	1.6E − 14	9.8E − 14
			2	2.4E − 13	3.6E − 12
CPS/RK	6	1E − 03	1	1.8E − 14	1.3E − 13
			2	3.4E − 13	8.9E − 12

Table 9
Error in the solution of the Lagrangian shallow water equations for the nonlinear test problem

Method	N, M	Δt	T	$e_\infty(x,y)$	$e_\infty(h)$
FD/FD	10	1E − 03	0.5	5.0E − 04	1.7E − 02
	22	1E − 05	0.5	8.3E − 06	5.7E − 03
	40	1E − 06	0.5	5.3E − 06	2.1E − 03
	40	1E − 04	1	3.2E − 04	2.7E − 02
CPS/RK	6	1.E − 03	0.5	2.7E − 05	5.2E − 02
	16	1E − 04	0.5	7.5E − 08	8.6E − 05
	32	1E − 05	0.5	2.3E − 12	1.7E − 09
	32	1E − 05	1	6.4E − 06	6.1E − 03

- *Nonlinear*

$$x = \frac{a\cos t - b\sin t}{\sqrt{a^2 + b^2 + \mathrm{e}^{-2t}(1 - a^2 - b^2)}},$$
$$y = \frac{a\sin t + b\cos t}{\sqrt{a^2 + b^2 + \mathrm{e}^{-2t}(1 - a^2 - b^2)}},$$
$$h = h_0\mathrm{e}^t(a^2 + b^2 + \mathrm{e}^{-2t}(1 - a^2 - b^2)).$$

As was the case with the spiral sink, we see exponentially growing values of h, so we again choose $h_0 = 2 \times 10^{-5}$. Solutions in the (xy)-plane with initial positions inside the unit circle spiral outward towards the circle, while initial positions outside the circle, spiral inward towards it. Our choice of domain results in both types of behavior (see Fig. 5).

Since both the spatial and temporal approximations are highly nonlinear, there is no benefit to studying the low order spatial approximation with the high order temporal approximations (FD/RK). In Table 9 we give results from both the high order and low order methods for increasing grid sizes. At time $T = 0.5$ we see the significant advantage of the high order spatial and temporal approximation. In addition, as we increase the number of grid points the accuracy of CPS/RK increases at a higher rate than with the low order (FD/FD) approximation. However at $T = 1.0$ the accuracy of both methods rapidly decay because again we have exponentially growing h.

4. Conclusions

We have derived, analyzed, and numerically solved the shallow water equations in Lagrangian coordinates when the underlying dynamical system possesses a center, source, saddle, spiral sink, and one case when the spatial flow is nonlinear. Lagrangian coordinates are often avoided because it is perceived that the domain may become too twisted or distorted for numerical approximation. If the Lagrangian form is transformed back to Eulerian form (as is the case with semi-Lagrangian or ALE methods) this is a problem. However, we calculate in a purely Lagrangian domain and the grid does not become twisted or distorted with time because the grid is the initial positions of the particles. The difficulty with solving purely in Lagrangian coordinates is that the corresponding partial differential equation is highly nonlinear and involves computing the inverse of the Jacobian, which is not possible if the Jacobian vanishes. Thus in is this work we explicitly state the Jacobian and determine that the Lagrangian shallow water equations are not valid for the following two cases: (1) the particles converge together and the isopycnal moves infinitely deep, and (2) the isopycnal is sufficiently deep initially but moves to the surface as the particles diverge as a source

(spiral) or saddle. In all other cases the shallow water equations can be solved in Lagrangian coordinates for long time periods. We also show that (linear) steady state solutions of the Lagrangian shallow water equations have Jacobian equal to one. Even though this analysis is for spatially linear flows, it gives us an indication of how the Lagrangian shallow water equations will behave locally for nonlinear flows.

When the Lagrangian shallow water equations are valid, or if the initial depth was chosen to be sufficiently small, accurate Lagrangian solutions were found with traditional Eulerian numerical methods. If the particles' positions change linearly with respect to their initial position, simple spatial derivative calculations result in errors of 10^{-13} after the flow had completed at least one cycle through the domain. When the relationship between the particles' position and their initial position is not linear, a high order spatial approximation should be used to get errors on the order of 10^{-13}. In either case, a high order temporal approximation such as the fourth order Runge–Kutta method used here, is needed to accurately solve the linear flow in Lagrangian coordinates.

In the nonlinear example, errors of the order 10^{-6} were obtained after a shorter time scale than in the linear examples. However, in this example the shallow water equations eventually became invalid. In order to have a thorough understanding of circulation in a purely Lagrangian reference frame, a similar analysis to the one done here will need to be carried out with the full primitive equations.

Acknowledgements

I thank the referee for useful comments which improved Sections 2 and 3.

References

[1] G.K. Batchelor, An Introduction to Fluid Dynamics, Cambridge University Press, Cambridge, 2000, p. 615.
[2] A.F. Bennett, B.S. Chua, Open boundary conditions for Lagrangian geophysical fluid dynamics, J. Comp. Phys. 153 (1999) 418–436.
[3] C. Canuto, M.Y. Hussaini, A. Quarteroni, T.A. Zang, Spectral Methods in Fluid Dynamics, Springer-Verlag, New York, 1988.
[4] B. Fornberg, A Practical Guide to Pseudospectral Methods, first ed., Cambridge University Press, New York, 1996.
[5] J.S. Hesthaven, P.G. Dinesen, J.P. Lynov, Spectral collocation time-domain modelling of diffractive optical elements, J. Comput. Phys. 155 (1999) 287–306.
[6] S.K. Kao, The Lagrangian Governing Equations of a Rotating, Compressible, Viscous Atmosphere, PAGEOPH, vol. 119, Birkhöuser Verlag, Basel, 9–15, 1980/81.
[7] A.J. Mariano, A. Griffa, T.M. Özgökmen, E. Zamianchi, Lagrangian analysis and predictability of coastal and ocean dynamics 2000, J. Atmos. Ocean. Tech. 19 (7) (2002) 1114–1126.
[8] L. Margolin, Introduction to arbitrary Lagrangian–Eulerian computing method for all flow speeds, J. Comp. Phys. 135 (1997) 198–202.
[9] J.L. Mead, R.A. Renaut, Accuracy of the modified Chebyshev method, SIAM J. Sci. Comput. 24 (1) (2002) 143–160.
[10] J.L. Mead, A.F. Bennett, Towards regional assimilation of Lagrangian data: The Lagrangian form of the shallow water reduced gravity model and its inverse, J. Marine Syst. 29 (2001) 365–384.
[11] M.N.L. Narasimhan, Principles of Continuum Mechanics, Wiley, 1992, p. 584.
[12] R. Renaut, J. Frohlich, A pseudospectral Chebyshev method for the 2D wave equation with domain stretching and absorbing boundary conditions, J. Comput. Phys. 124 (1996) 324–336.
[13] R. Renaut, Stability of a Chebychev pseudospectral solution of the wave equation with absorbing boundaries, J. Comput. Appl. Math. 87 (1997) 243–259.
[14] A. Staniforth, Côteé, Semi-Lagrangian integration schemes for atmospheric models – a review, Mon. Wea. Rev. 119 (1991) 2080–2206.
[15] H. Tennekes, J.L. Lumley, A First Course in Turbulence, MIT Press, Cambridge, 1972, p. 300.
[16] J.-Y Yang, C.A. Hsu, W.H. Hui, A Generalized Lagrangian method for solving the steady shallow water equations, Math. Comput. Simul. 35 (1993) 43–61.